Poly(D,L-Lactic Acid) (PDLLA) Biodegradable and Biocompatible Polymer Optical Fiber

Agnieszka Gierej, Maxime Vagenende, Adam Filipkowski, Bartlomiej Siwicki, Ryszard Buczynski, Hugo Thienpont, *Member, IEEE*, Sandra Van Vlierberghe, Thomas Geernaert, Peter Dubruel, and Francis Berghmans, *Senior Member, IEEE*

***Abstract*—We demonstrate that commercially available poly(D,L-lactic acid) (PDLLA) is a suitable material for the fabrication of biodegradable optical fibers with a standard heat drawing process. To do so we report on the chemical and optical characterization of the material. We address the influence of the polymer processing on the molecular weight and thermal properties of the polymer following the preparation of the polymer preforms and the fiber optic drawing process. We show that cutback measurements of the first optical fibers drawn from PDLLA return an attenuation coefficient as low as 0.11 dB/cm at 772 nm, which is the lowest loss reported this far for optical fibers drawn from bio-resorbable material. We also report on the dispersion characteristics of PDLLA, and we find that the thermo-optic coefficient is in the range of -10^{-4}°C^{-1}. Finally, we studied the degradation of PDLLA fibers in vitro, revealing that fibers with the largest diameter of 600 μm degrade faster than those with smaller diameters of 300 and 200 μm and feature more than 84% molecular weight loss over a period of 3 months. The evolution of the optical loss of the fibers as a function of time during immersion in phosphate-buffered saline indicates that these devices are potential candidates for use in photodynamic therapy-like application scenarios.**

***Index Terms*—Biodegradable materials, optical polymers, plastic optical fiber.**

Manuscript received October 25, 2018; revised December 24, 2018; accepted January 20, 2019. Date of publication January 31, 2019; date of current version April 11, 2019. This work was supported in part by the Research Foundation Flanders (FWO) project under Grant G048915N "Biodegradable Fiber Optic Technology for Biophotonic Applications" and Grant G0F6218N (EOS-convention 30467715), in part by the FWO project FWOKN273 to the Polymer Chemistry and Biomaterials Group, Universiteit Gent, and in part by the Polish National Science Centre through project HARMONIA under Grant UMO-2013/10/M/ST3/00708 to the Institute of Electronic Materials Technology. *(Agnieszka Gierej and Maxime Vagenende contributed equally to this work.) (Corresponding author: Agnieszka Gierej.)*

A. Gierej, M. Vagenende, and S. Van Vlierberghe are with the Department of Applied Physics and Photonics, Vrije Universiteit Brussel, Brussels Photonics, Brussels B-1050, Belgium, and also with the Department of Organic and Macromolecular Chemistry, Polymer Chemistry and Biomaterials Group, Centre of Macromolecular Chemistry, Universiteit Gent, Ghent B-9000, Belgium (e-mail: agnieszka.gierej@vub.be).

A. Filipkowski, B. Siwicki, and R. Buczynski are with the Institute of Electronic Materials Technology, Warszawa 01-919, Poland.

H. Thienpont, T. Geernaert, and F. Berghmans are with the Department of Applied Physics and Photonics, Vrije Universiteit Brussel, Brussels Photonics, Brussels B-1050, Belgium.

P. Dubruel is with the Department of Organic and Macromolecular Chemistry, Polymer Chemistry and Biomaterials Group, Centre of Macromolecular Chemistry, Universiteit Gent, Ghent B-9000, Belgium.

Digital Object Identifier 10.1109/JLT.2019.2895220

I. Introduction

BIOCOMPATIBLE and biodegradable optical waveguides and photonic devices have recently gained increased attention owing to their potential for application in the biomedical field. Before proceeding, we clarify what we mean when referring to biodegradable and biocompatible materials. Depending on the research field, the term "biodegradation" can be interpreted in different ways. In the biomedical field, biodegradable polymers are applied as sutures, implants or for applications in drug delivery, amongst others. The term biodegradation refers to cleavage of the polymer backbone, i.e., chemical decomposition, as a result of the interaction with biological substances. The latter can include, for example, enzymes, secretion products or living organisms, fungi or bacteria. On the other hand, when talking about biocompatibility, we refer to a material that elicits an appropriate biological response upon implantation in the body such that it can be used for long-term contact with living tissues and hence co-exist with these without causing an unacceptable degree of harm to the human body [1]. Biocompatibility of a material indicates not only the absence of cytotoxicity but also enables a device made from that material to perform to its full potential at the implant site [2].

Waveguides made from biodegradable and biocompatible materials can behave in a bio- and eco-friendly manner, can be produced at relatively low cost, and their properties can be adjusted by ways of a tailored waveguide geometry supplemented with doping and chemical functionalization [3]–[5]. Functionalizing or doping the material should nevertheless be done such that supplementary materials do not compromise the biodegradability and biocompatibility. One class of applications, for which such waveguides could provide unprecedented features, pertains to light delivery inside a patient's body. Light-based *in vivo* therapies currently require invasive treatments involving either regular or keyhole surgery [6]. The use of biodegradable optical fibers which can be implanted in a patient's body during the required treatment period and which can be used multiple times, as well as left in the body after treatment and allowed to degrade naturally, would enable much less invasive therapies.

Several authors previously reported on the possible use of synthetic and biocompatible materials for optical and biomedical applications [7], [8]. A first yet peculiar structured polymer optical fiber made from two types of biodegradable cellulose has been reported already a decade ago [4]. Other

polymers have also been investigated to function as biocompatible photonic devices, such as 3D printed silk waveguides and step index silk optical waveguides [5], [9]. Calcium-phosphate glass based resorbable optical fiber was also reported as a candidate for biomedical applications [10]. Light-guiding hydrogel waveguides have been proposed for sensing [11] and photodynamic therapy[12]. Poly(L-lactic acid) (PLA) and poly(D,L-lactide-co-glycolide) (PLGA) tested in the shape of a slab were proposed for controlled light delivery and photochemical tissue bonding (PTB) [13]. A biodegradable citrate-based step index polymer fiber was proposed for organ-scale light delivery and collection [14]. Very recently, poly(L-lactic acid) (PLLA) was also transformed into fibers, which were implanted to study deep-brain neural activity. In this work, the authors demonstrated that PLA-based polymers exhibit desirable features such as controllable processability to serve as biodegradable optical waveguides [15].

The above prompted us to consider the use of another lactic acid based polymer, i.e., poly(D,L-lactic acid), abbreviated as PDLLA, for the production of actual optical fibers for biomedical applications. PDLLA has been investigated already as scaffold material for tissue engineering [16], [17], as filaments for controlled drug delivery [18] and recently also in the form of synthetic nerve conduits composed of PDLLA/β-TCP/ collagen for peripheral nerve regeneration [19]. PDLLA is a well-known commercially available amorphous polyester. It is biocompatible and known to degrade *in vivo* over time due to hydrolytic degradation or biodegradation through cleavage of its backbone ester linkages [17], with a degradation time that depends on the thickness and morphology of the polymer sample and on the implantation site [20]. These features, together with the anticipated adequate processability, mechanical strength, thermomechanical stability and optical transparency made us select PDLLA as candidate material for the fabrication of optical fibers. We believe that PDLLA may be better suited for optical fiber fabrication since, in contrast to PLLA, it is an amorphous material, which indicates that lower optical loss could be achieved. The polymer processing temperature of PDLLA can also be lower than that of PLLA, which implies that thermal degradation can be limited as well. Owing to these properties and to its glass transition temperature (Tg) exceeding the physiological temperature of 37 °C, PDLLA can be envisaged for *in vivo* applications using fibers made from this material.

We have structured our manuscript as follows. Section II describes bulk PDLLA and deals with both the chemical and optical characteristics of this material. We report data on optical attenuation as a function of wavelength and compare the value to that of bulk PMMA at selected wavelengths. We also show the dispersion profile and estimate the thermo-optic and thermal expansion coefficients. Section III deals with the results following preform preparation and heat drawing of preforms into fibers. We study the influence of the fabrication process on the thermo-mechanical and physico-chemical properties of the polymer by comparing the T_g values, as well as mass loss of the granulate, preforms and produced fiber. Moreover, we report on the *in vitro* degradation of our fibers over a period of 3 months. Subsequently, we focus on the optical attenuation of PDLLA fibers from two fabrication batches, as measured by a conventional cutback method. We also report on the evolution of optical loss as a function of time induced in unclad PDLLA fiber following immersion in phosphate-buffered saline. We close our manuscript with Section IV, including a summary of our findings supplemented with perspectives for future research.

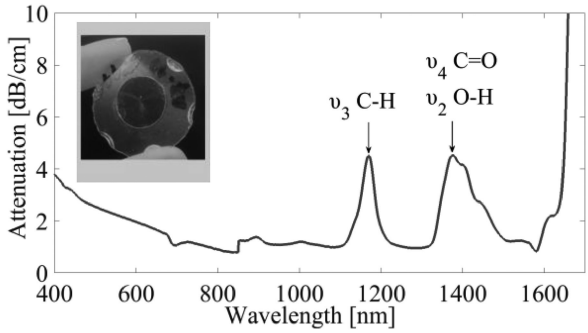

Fig. 1. Attenuation expressed in dB/cm of a PDLLA bulk sample fabricated by compression molding. The inset shows a photograph of the sample.

II. Chemical and Optical Characterization of Purchased and Plate Processed PDLLA

We purchased PDLLA (PURASORB PDL 20) with an inherent viscosity of 2.0 dl/g in the form of granulate from Corbion Purac Biomaterials [21]. The PURASORB products are regulated by the Food and Drug Administration (FDA) and registered under FDA number DMF-21817 [22].

We confirmed the chemical structure and purity of the product by ^{1}H-NMR spectroscopy using a Bruker Avance 300 MHz Ultrashield NMR spectrometer and via attenuated total reflectance - Fourier transform infrared spectroscopy (ATR-FT-IR) using a Biorad FT-IR spectrometer FTS 575C. The granulate had a T_g of 50 °C, which we determined by differential scanning calorimetry (DSC) using a TA instrument Q2000 DSC device. We also determined the number average molecular weight (Mn) of the granulate by size exclusion chromatography (SEC) on a Waters GPC Alliance 2695 to be 260 kg/mol, with a polydispersity of 1.13. The degradation temperature of the granulate was 365 °C, as we determined via thermogravimetrical analysis (TGA) using a TA Instruments Q50 device.

Before we processed the PDLLA into preforms and optical fibers, we produced flat PDLLA plates with the aim to assess the optical transmittance of the bulk polymer in the VIS-NIR region. We used a compression molding device (Jenoptik HEX04) to fabricate samples with uniform thickness and low surface roughness. We used varying amounts of PDLLA granulates to obtain plates with different thicknesses. The compression molding was performed under vacuum to prevent thermo-oxidative degradation [23]. We obtained transparent polymer plates with a diameter of 15 mm and thicknesses of 0.65 to 1.00 mm (see Fig. 1), using 0.3 to 0.6 g of granulates.

Following the production of the PDLLA samples, we measured their optical transmission and specular reflectance spectra with a double beam Jasco V670-EX Spectrophotometer.

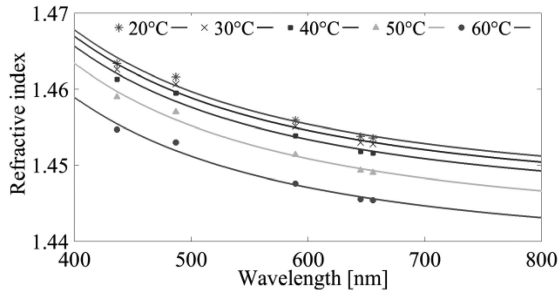

Fig. 2. PDLLA refractive index measured at different temperatures (dots) and Sellmeier equation fits (solid lines).

Fig. 1, shows a recorded attenuation spectrum in the VIS-NIR wavelength region measured on a sample with a 0.932 mm thickness. Three normal overtones corresponding to the symmetric and asymmetric stretching and deformation vibrations v_3 C-H, v_4 C = O and v_2 O-H are clearly present at 1170, 1380 and 1400–1440 nm, respectively [24]. We find attenuation values at typical polymer optical fiber transmission wavelengths of 1.78 dB/cm and 0.94 dB/cm at 633 nm and 800 nm, respectively. Note that these are substantially larger than those of poly(methyl methacrylate) (PMMA), which is conventionally used as a basis for polymer optical fibers, with reported loss values at 633 nm between 0.04 dB/cm for a low-cost extruded bulk rod to 0.007 dB/cm for a high-purity cast PMMA rod [25]. We also observe an interesting low loss window covering the 1550–1580 nm region, with losses of 1.21 down to 0.82 dB/cm.

For the sake of comparison, in the same wavelength region, the intrinsic absorption of PMMA is $10^{-0.5}$ cm^{-1} and the attenuation is around 1.36 dB/cm [26], [27].

These results indicate that the as-processed PDLLA features optical loss levels in the VIS-NIR wavelength region that allow considering its use for fiber fabrication. Optical loss values of around 1 dB/cm would indeed still be compatible with *in vivo* applications, projecting that only relatively short fiber lengths of maximum a few tens of cm would be required for such purposes (see also Section III-D).

An additional parameter of interest is the refractive index and the dispersion of the material, as well as the thermo-optic coefficient when considering, for example, optical fiber sensor applications. We measured the refractive index of the bulk samples in the VIS spectral range using an Anton Paar Abbemat MW Refractometer at 5 wavelengths in the range of 436 to 656 nm. During the measurements, the temperature was controlled by means of a built-in Peltier thermostat in the range from 20 to 60°C. Fig. 2 shows the measurement results and, to the best of our knowledge, this represents the first measurement of the dispersion curve and thermo-optic characteristics of PDLLA. The refractive index follows a regular dispersion profile for temperatures below T_g. The data was fitted to the Sellmeier dispersion formula [26]. When the material reaches 40°C and as the temperature continues to increase beyond the T_g, we observe a characteristic pronounced decrease of the refractive index.

For all the wavelengths and in the temperature range below T_g, the thermo-optic coefficient equals -1.0×10^{-4} °C^{-1}. PDLLA thus fits within the group of glassy polymers, such as PMMA, which have dn / dT values in the range of -1– -2×10^{-4} °C^{-1} [28]. From the measurements, we can also estimate the thermal volumetric expansion coefficient, using the Lorentz–Lorenz relation given in (1), which relates the refractive index with temperature at values below T_g [29] as follows:

$$\frac{n^2+2}{n^2-1} = aT + b \tag{1}$$

and with $\beta = a / b$ We estimated that β lies within the range 1.92–2.00 $\times 10^{-4}$°C^{-1}. This is not that far off from values reported for PMMA, either i.e., 2.20–2.70 $\times 10^{-4}$°C^{-1} [27]. This thermal expansion coefficient and the thermo-optic coefficient provide useful information, for example in view of the manufacturing of the preforms, as well as in view of possible sensor applications of PDLLA based optical fibers.

III. Optical and Chemical Characterization of Heat-Drawn Unclad Fibers

A. Fiber Drawing

To fabricate the fiber preforms, we used a melt-casting process in dedicated Teflon molds with an internal diameter of 13 mm. We filled the molds with PDLLA granulate and placed them in a vacuum oven at 180 °C for several hours, until the material was fully molten after which the molds were refilled with additional PDLLA granulate. Note that no pressure was applied to the melt leading to the appearance of vacuum voids due to shrinkage of the material upon cooling. Yet the void-free portions were sufficiently large to consider drawing the preform with an eventual diameter of 12.5 mm and a length of 150 mm into an optical fiber.

We produced the PDLLA fibers from the preform discussed above with a standard heat drawing procedure [30]. We fabricated two batches of PDLLA fibers successfully using two different drawing towers with different furnace dimensions. The first batch was drawn using a furnace with a diameter of around 3 cm at approximately 122 °C and the second using a furnace with a diameter of about 5 cm at 130 °C, after heating the preforms up to 100 °C at a rate of 5 °C/min. Note that these are furnace temperatures measured using thermocouples. They do not correspond to actual material temperatures. The levels were set empirically by increasing the temperature up to the point where the polymer softened sufficiently and appeared ready to be drawn. From there onwards, the furnace temperature was not raised any further to avoid thermal degradation.

We flushed with N_2 to avoid oxidation of the polymer. To initiate the drawing, we attached weights of 440 g to the bottom of the preform when the material had reached the correct drawing temperature. Once the drawing process was initiated, we reduced the weight to 180 g for the drawn fiber to reach a sufficient length to be taken up by the draw tower capstan, allowing for draw tension control. Consecutively, several meters of unclad fiber were obtained, which were collected by an automatically spinning capstan that allowed controlling the drawing speed. Varying this speed between 0.5 to 2 m/min resulted in fibers with controllable diameter from 2 mm down to 120 μm.

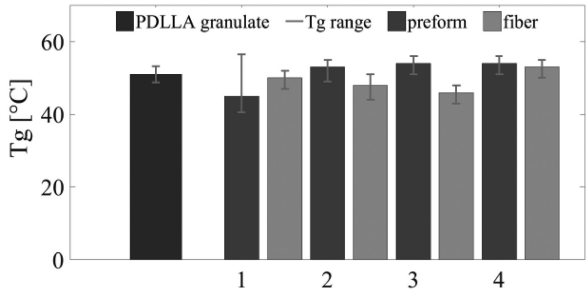

Fig. 3. Comparison of T_g values and indication of the T_g ranges for PDLLA granulate, 4 preforms (indicated with a number in the graph) and the corresponding heat-drawn fibers from the second batch.

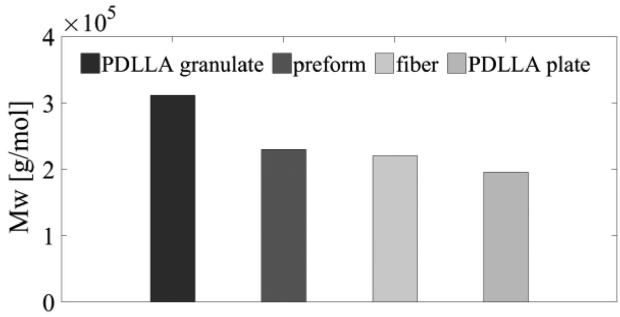

Fig. 4. Average Mw values for PDLLA granulates, preforms, corresponding fibers from the second batch and compression molded PDLLA plate.

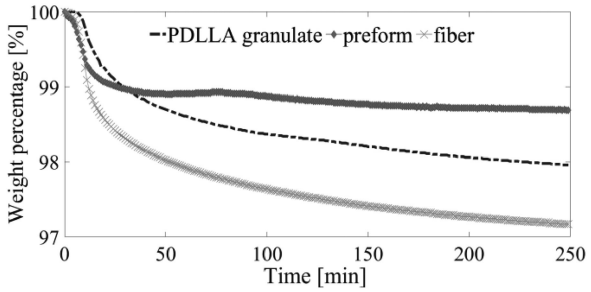

Fig. 5. Mass evolution of PDLLA granulate, preform 4 and fiber 4 (second batch) as a function of time at a temperature of 130 °C, as studied using TGA.

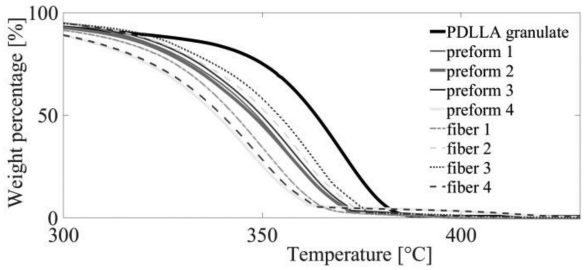

Fig. 6. Mass evolution of PDLLA granulate, preforms and fibers as a function of temperature, studied using TGA.

We measured the unclad fiber outer surface roughness using a Bruker Contour GT-I Optical Microscope. The average of 10 measurements performed along 10 cm of a representative PDLLA fiber returned a root mean square roughness Sq = 80 nm. For sake of comparison, we measured the roughness for a commercially available standard fiber GI PMMA 120 (purchased from Thorlabs [31]) with the same equipment to be Sq = 35 nm, which indicates that whilst there is room for improvement by means of a better control over the preform fabrication, the first drawing provides relatively smooth outer surfaces. Control over the surface roughness is important in view of the future fabrication of core-cladding structures with this material and the need to limit scattering loss at the core-cladding interface [32].

B. Chemical Characterization

Following their fabrication, we analyzed both the PDLLA preforms and fibers with SEC, TGA and DSC to investigate the influence of the fabrication process on the thermo-mechanical and physico-chemical properties of the polymer. This was done to assess the potential temperature processing range of the material as well as the effect of the processing on the thermomechanical properties of the material. DSC showed that the T_g of the material remained almost unchanged (the largest observed difference of 6 °C) after processing into a preform, as depicted in Fig. 3.

SEC indicated that the average Mw for the PDLLA preforms was around 230 000 g/mol (dispersity = 1.2) and the average Mw for the corresponding fibers was 220 000 g/mol (dispersity = 1.1). This means that the fiber drawing of PDLLA did not result in any substantial molecular weight loss (see Fig. 4). The first processing step of PDLLA, i.e., melting the granulates into preforms, resulted in a 26% Mw loss. The Mw remains more than sufficiently large for the material to remain processable. Note that we observed more mass reduction (37%) in the PDLLA plates which indicates that differences in processing temperature and applied force lead to samples with different characteristics and hence that the properties of the fibers and plates cannot be straightforwardly compared.

Besides the molecular weight, we also monitored the mass of the granulate, remnant of the undrawn preform and fiber, at a constant temperature of 130 °C (equal to the fiber drawing temperature) using TGA to investigate the potential mass loss that occurs during the material processing. After 4 hours storage at 130 °C, we observed mass losses ranging between 1.3 and 2.8% (see Fig. 5). The drawing process only resulted in a weight loss of the fiber, while the degradation temperature of the product remained unaffected, as illustrated in Fig. 6.

The fact that fibers could be produced from multiple PDLLA preforms, using two different drawing towers with different furnace dimensions and that the obtained preforms and fibers have similar physico-chemical properties and display limited molecular weight loss indicates that heat-drawing of PDLLA is a repeatable process.

C. Degradation Study

Upon exposure to the aqueous environment in the human body, polyesters such as PDLLA degrade into oligomers (and eventually into lactic acid) that can be metabolized via natural pathways. The degradation behavior of polymers can be tested *in vitro* to predict their behavior when implanted. To

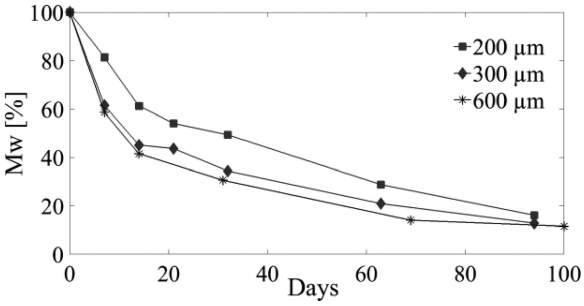

Fig. 7. Mw percentage of PDLLA fibers immersed in PBS at 37 °C as a function of time.

test for biodegradability, biomaterials are usually incubated in phosphate-buffered saline (PBS), with or without enzymes, at 37°C to simulate the *in vivo* conditions. We did so as well for the purpose of our study and for confirming the degradation of unclad PDLLA fiber. More specifically, we evaluated the biodegradability of both batches of fabricated PDLLA fibers in a simulated biological environment [33] to confirm that degradation occurs, and we based our assessment on the measured changes in molecular weight.

To do so we immersed fibers with diameters of 200, 300 and 600 μm in phosphate-buffered saline (PBS) (0.1 M, pH = 7.4), and we subsequently incubated at 37 °C for a period of about 3 months. The PBS was renewed every week. We analyzed the molecular weight (Mw) of the fibers using SEC on a Waters GPC Alliance 2695 every week during the first month and every 30 days thereafter. Fig. 7 shows the degradation expressed as the remaining molecular weight of the PDLLA fibers as a function of time.

After the first two weeks, we observe a pronounced decrease of the molecular weights down to 61, 45 and 41% of the initial values for the 200 μm, 300 μm and 600 μm diameter fibers, respectively. After approximately 100 days, the remaining molecular weights are 16, 13, 12% of the initial values for the 200, 300 and 600 μm diameter fibers, respectively. These values agree well with those reported for the degradation of PDLLA plates, for which the remaining Mw was 10% after 14 weeks [34].

During the first days, we could observe a change of appearance from transparent to white and swelling of the samples due to water uptake. More specifically, we observe a pronounced length reduction of the filaments along with a substantial increase in their width along with water uptake. These observations have also been reported by Heidemann *et al.* [35] who investigated the degradation of PDLLA implants *in vivo*.

The PBS solution penetrates the polymer matrix and as a result the cleavage of the covalent bonds in the polymer backbone is initiated in the hydrated region of the PDLLA fibers, which leads to a decrease of the molecular weight as clearly measured during the first two weeks. As the degradation continues, the newly formed carboxylic acid end groups of the polymers accelerate the polymer chain scissions by end-group mediated autocatalysis. Further stages of the degradation process lead to complete erosion and full loss of the integrity of the samples [34]. At the end of the degradation study the samples appeared porous and the lower diameter fibers were randomly coiled, but their mechanical integrity was still sufficient to manipulate them without specific care.

Note that the degradation of PDLLA fibers stems from a combination of bulk diffusion, surface diffusion, bulk erosion and surface erosion. Fig. 7 reveals that the degradation rate of PDLLA fibers depends on their diameter. The thicker the fiber, the faster the degradation. This indicates that the degradation in the bulk happens faster than at the surface with accelerated degradation in the center due to a negative gradient of the penetrating water concentrations from the surface to the sample's center, as previously reported [34]. The dependence of the degradation rate on the sample geometry suggests that the fiber diameter could be adapted to match a desired degradation period, which may be important, for example, in view of applications involving fiber-based drug release.

It is nevertheless challenging to predict the degradation rate of the PDLLA fibers *in vivo*. We can expect a higher degradation rate owing to the dynamic environment of an *in vivo* system. Living organisms provide for additional factors that can accelerate the decomposition. *In vivo*, the degradation of aliphatic polyesters is readily hydrolyzed by water-soluble enzyme, lipases [36]. The enzymes activity, their concentration in human serum and their action may affect the degradation rate. Additionally, the foreign body response results in the accumulations of cells such as of macrophages around the sample. Free radicals, acidic products, or enzymes produced by these cells during the foreign body response may also accelerate degradation [37]. It has to be highlighted as well that the magnitude of tissue response to a resorbable material depends to a great extent upon the site of the implantation [38]. The aim would be to consider all these factors in view of controlling the biodegradation rate. We forecast that a PDLLA fiber could perform its function *in vivo* during a period up to approximately two months.

Although experiments that demonstrate actual *in vivo* biocompatibility and biodegradability of our unclad PDLLA fibers are not presented here, we recall that PDLLA has been extensively studied in terms of biomedical and pharmaceutical applications and used for the development of medical devices. Moreover, it has been demonstrated that PDLLA has no toxic effect on pneumocytes [17] and PDLLA polymeric films implanted after the sciatic nerve transection and anastomosis caused no inflammation or tissue damage in various organs in rats [20]. In addition, three cases regarding clinical degradation and biocompatibility of PDLLA in human body have been reported where no clinical signs of foreign-body reactions could be found [39].

D. Optical Characterization

We measured the attenuation of PDLLA unclad fibers from the two fabrication batches with various outer diameters at a wavelength of 633 nm using the well-known cutback method [40]. Before the measurements, we cleaned the fiber with isopropyl alcohol to remove impurities from its outer surface. We cleaved the fiber ends using a microtome blade on a hot plate kept at around 27–30 °C. Fig. 8(a) illustrates the results of such

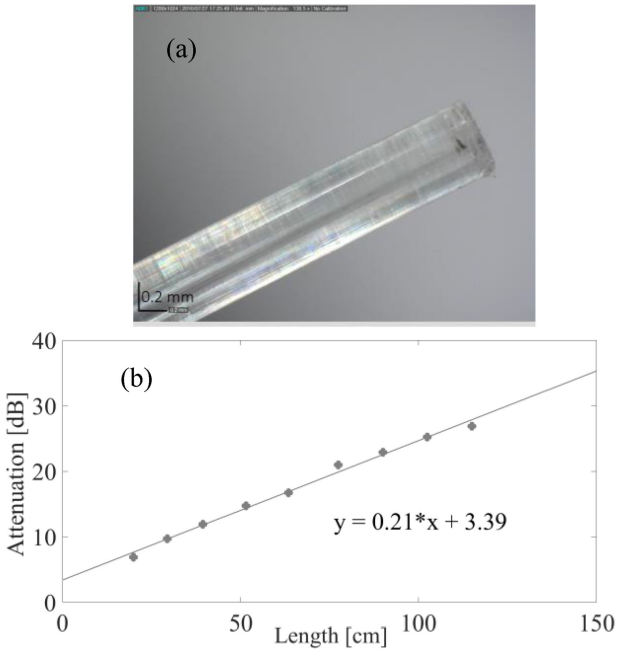

Fig. 8. (a) Hot blade cut end of a PDLLA unclad fiber with a diameter of 590 μm. (b) Cutback measurement at 633 nm revealing an attenuation of 0.21 dB/cm calculated using a linear regression (solid line) with R^2 value of 0.99.

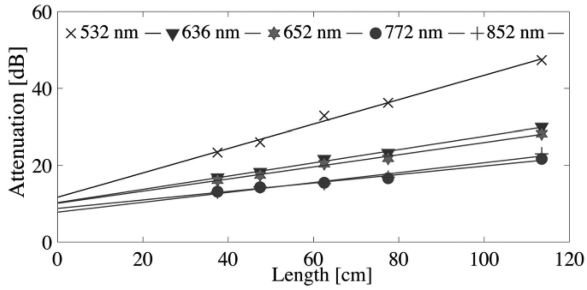

Fig. 9. Spectral cutback measurements at selected wavelengths carried out with a broadband source and optical spectrum analyzer on an as-drawn PDLLA unclad fiber (1st batch) with an averaged diameter of 550 μm. The solid lines are the linear regressions, the slope of which returns the attenuation in dB/cm.

a cleaving procedure. Fig. 7(b) shows the attenuation at $\lambda = 633$ nm (from a HeNe laser) of a fiber from the first batch measured with an initial fiber length of 115 cm of which we successively cut portions of 12 cm. The measured diameter averaged over 1 m of fiber length was $\phi = 590 \pm 59$ μm.

We also measured the attenuation of PDLLA fiber from the first batch with an averaged diameter of 550 ± 38 μm using a broadband Halogen source and an Instrument Systems SPECTRO 320 optical spectrum analyzer. Fig. 9 shows the results at several selected wavelengths. At typical POF transmission windows around 650 nm and 850 nm, we obtain attenuations of 0.16 dB/cm and 0.13 dB/cm respectively. We find the lowest attenuation of $\alpha = 0.11$ dB/cm at 772 nm. Note that in these wavelength regions the fiber loss is significantly lower than the attenuation measured with the PDDLA plates discussed in Section II. This stems from the different processing conditions used to fabricate plates and fibers (see also our earlier comment pertaining to the different characteristics) and the extrinsic losses due to scattering centers and impurities introduced during the fabrication of the plates. We nevertheless find the lowest loss in the region around 780 nm, which is in line with the low loss in the 780–850 nm region of the PDLLA bulk samples (see also Fig. 1).

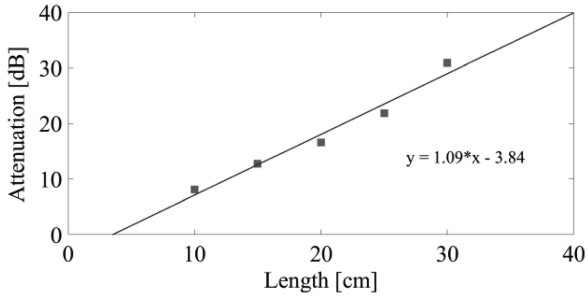

Fig. 10. Cut-back measurement on an unclad PDLLA fiber (2nd batch) at 1580 nm revealing an attenuation of 1.1 dB/cm. The R^2 value of the linear regression is 0.97.

In the attenuation spectrum shown in Fig. 1, we also note that bulk PDLLA exhibits a low loss window covering the 1550–1580 nm region. We therefore also measured the loss of PDLLA unclad fibers using the cut-back method at 1580 nm with a TSL-710 Santec tunable laser and Newport 918D-IR-OD3R Germanium Photodetector. Fig. 10 shows that the attenuation at that wavelength is about 1.1 dB/cm for fiber with a diameter of 550 ± 40 μm. This value agrees with the level of the attenuation of the bulk material at that wavelength in Fig. 1.

For sake of comparison, the theoretical loss limit of PMMA optical fiber is 0.00106 dB/cm in the transmission window around 650 nm [41]. Although, the attenuation of unclad PDLLA at that wavelength is three orders of magnitude above that of commercially available PMMA POFs, typical application scenarios for PDLLA fibers are not limited by this loss since only short fiber lengths will be required. To illustrate this, we take the case of *in vivo* light delivery system for photodynamic therapy (PDT). PDT uses photosensitizers that are activated by absorption at visible wavelengths, e.g., methylene blue at 655 nm and porphyrin at 630 nm. The length of optical fibers used for PDT purposes can vary. Fibers utilized for PDT of head and neck malignancies were 10–15 cm long [42]. For interstitial treatments, a cylindrically-diffusing fiber is often used so that it can irradiate a larger volume of tissue. Commercially available fibers (e.g., manufactured by Medlight, Lausanne, Switzerland) have a stripped cladding and their core is coated with a light-scattering material along the desired length of the diffusing tip. They are available in lengths up to 5–10 cm, and have an outside tip diameters of 1 mm [43]. If we therefore assume useful lengths of 10 cm and a POF connector loss of 1.5 dB [44], the total insertion loss of the device will be around 3.6 dB at a wavelength of 633 nm.

Fig. 11 depicts the attenuation in the VIS and NIR region of the 550 μm diameter fiber and reveals the intrinsic absorption maxima at 736 and 627 nm, which are due to the presence of

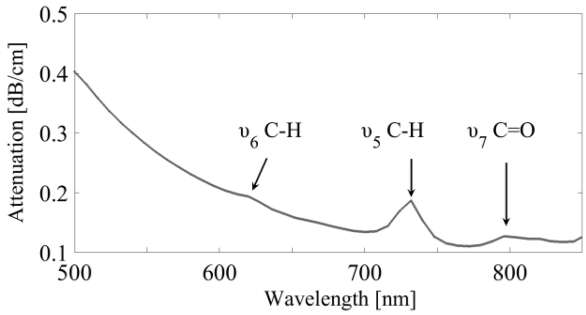

Fig. 11. Spectral attenuation of the as-drawn PDLLA fiber (first batch) with lowest loss of 0.11 dB/cm at 772 nm and indication of the absorption peaks.

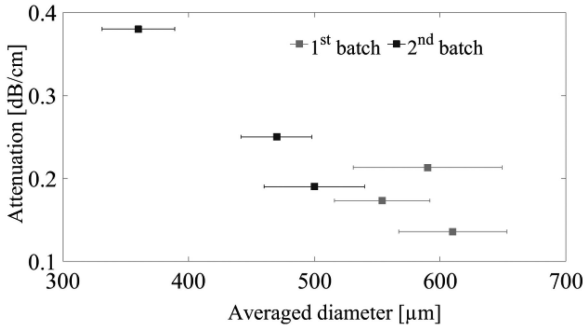

Fig. 12. Summary of the attenuation at 633 nm taken from single wavelength and broadband measurements for various averaged PDLLA fiber diameters taken from both the 1st and 2nd batches.

C-H stretching vibration overtones, whilst the C = O overtone can be spotted at 806 nm [24].

The attenuation at 633 nm for both the first and second batch PDLLA fibers with varying diameters are summarized in Fig. 12. The decreasing trend of attenuation with the unclad fiber diameter can be understood from the decreasing number of reflections at the waveguide-air interface with increasing diameter for a given fiber length, as explained for example in [45].

We have also studied the evolution of induced losses with immersion time in PBS at 37°C and pH = 7.4 of two unclad PDLLA fibers in a scenario representative for PDT. We coupled light from a HeNe laser at 633 nm into the fibers and we measured the power output using a Newport 918D-UV-OD3 Silicon Photodetector. We immersed a portion with a length of around 10 centimetres of a total 60 cm long fiber. The fibers had average diameters of 588 ± 41 μm and 523 ± 41 μm, respectively.

The Immersion Induced Loss (IIL) was calculated as follows:

$$IIL = \frac{10}{L} * \log_{10} \frac{P(t=0)}{P(t)} \tag{2}$$

where P is the measured optical power exiting the fiber, t is time and L is the length of the immersed fiber portion. The first sample (label IIL_1) was left in PBS in an unsupported manner, whilst the second (label IIL_2) was kept under slight tension to avoid bending.

Fig. 13 shows the ILL values for both PDLLA fibers as a function of immersion time. During the initial 60 min there is no presence of any additional loss. IIL_1 appears less steady than

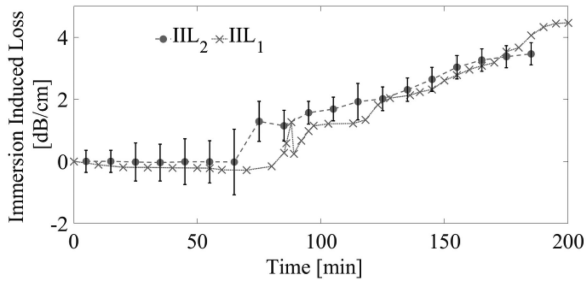

Fig. 13. Immersion induced loss (IIL) of unclad PDLLA fibers soaked in PBS at 37° as a function of immersion time. IIL_1 corresponds to the unsupported fiber and IIL_2 corresponds to the fiber kept straight. The error bars accounting for the standard deviation on averaged power measurements and for the uncertainty on the immersed fiber length are plotted for IIL_2. The dashed lines serve as a guide to the eye only.

IIL_2 which is likely due to coiling of the immersed fiber portion, but regardless of whether the fiber was left unsupported or kept straight, we observe a similar gradual loss increase with time.

Typical PDT application scenarios involve optical energy delivery times of 30 minutes [46]. Unclad PDLLA fiber would therefore still be fully-functional during such treatment. The application time can likely be extended by working with a fully-fledged step-index fiber.

IV. Conclusion

In conclusion, we demonstrated the possibility of processing commercially available PDLLA granulate into preforms and subsequently into unclad optical fibers via a repeatable heat-drawing procedure. We achieved biodegradable PDLLA fibers with an attenuation of 0.11 dB/cm at 772 nm, which is lower than that reported so far for other polymer biocompatible waveguides [4], [12]–[15].

We anticipate that by optimizing the preform fabrication and tailoring the composition and therefore the refractive index of the material, core-cladding structures can be obtained that would lead to practical devices and may reveal even lower attenuation values. For manufacturing a fully-fledged biodegradable step-index optical fiber we could envisage the use of other traditional synthetic polyesters such as poly-lactic-co-glycolic acid (PLGA), which has similar chemical properties but a different refractive index. We project that it is also possible to employ biocompatible hydrogels. These water-soluble polymers are non-toxic and have already been used for the manufacturing of optical fibers [12] and in the form of coatings [47]. Moreover, the experience with the processing of the material and the observed limited effect of the preform fabrication and fiber drawing on the physico-chemical characteristics of the polymer also allows envisaging the production of microstructured fibers.

We confirmed the *in vitro* degradation of the fabricated PDLLA fibers with a decrease of the molecular weights down to 16 %. 13%, 12% of the original values for 200, 300 and 600 μm diameter fibers, respectively, after 3 months incubation in PBS. We have also measured the evolution of optical loss at 633 nm of these unclad fibers during immersion in PBS, confirming that it can efficiently deliver light over a time period commensurate with that required for photodynamic therapy.

The biodegradable nature of the material, combined with the optical properties of the produced fibers, allows envisaging the fabrication of a fully-fledged polymer optical fiber that can be used to deliver light *in vivo* for periods of several hours and that can be left inside the body to degrade over a period of up to two to three months.

REFERENCES

[1] D. F. Williams, "On the mechanisms of biocompatibility," *Biomaterials*, vol. 29, no. 20, pp. 2941–2953, 2008.

[2] Y. Onuki, U. Bhardwaj, F. Papadimitrakopoulos, and D. J. Burgess, "A review of the biocompatibility of implantable devices: Current challenges to overcome foreign body response," *J. Diabetes Sci. Technol.*, vol. 2, no. 6, pp. 1003–1015, 2008.

[3] A. Dupuis *et al.*, "Biodegradable, double-core, porous optical fiber for sensing applications," in *Proc. Opt. Fiber Sensors, OSA Tech. Digest*, 2006, Art. no. WA2.

[4] A. Dupuis *et al.*, "Prospective for biodegradable microstructured optical fibers," *Opt. Lett.*, vol. 32, no. 2, pp. 109–111, 2007.

[5] M. B. Applegate, G. Perotto, D. L. Kaplan, and F. G. Omenetto, "Biocompatible silk step-index optical waveguides," *Biomed. Opt. Express*, vol. 6, no. 11, pp. 4221–4227, 2015.

[6] M. C. Derosa and R. J. Crutchley, "Photosensitized singlet oxygen and its applications," *Coordination Chem. Rev.*, vol. 234, pp. 351–371, 2002.

[7] S. Doppalapudi, A. Jain, W. Khan, and A. J. Domb, "Biodegradable polymers – An overview," *Polym. Adv. Technol.*, vol. 25, pp. 427–435, 2014.

[8] A. J. R. Lasprilla, G. A. R. Martinez, B. H. Lunelli, A. L. Jardini, and R. M. Filho, "Poly-lactic acid synthesis for application in biomedical devices – A review," *Biotechnol. Adv.*, vol. 30, no. 1, pp. 321–328, 2012.

[9] S. T. Parker *et al.*, "Biocompatible silk printed optical waveguides," *Adv. Mater.*, vol. 21, no. 23, pp. 2411–2415, 2009.

[10] E. Ceci-Ginistrelli *et al.*, "Novel biocompatible and resorbable UV-transparent phosphate glass based optical fiber," *Opt. Mater. Express*, vol. 6, no. 6, pp. 2040–2051, 2016.

[11] M. Choi, J. W. Choi, S. Kim, S. Nizamoglu, S. K. Hahn, and S. H. Yun, "Light-guiding hydrogels for cell-based sensing and optogenetic synthesis in vivo," *Nature Photon.*, vol. 7, no. 12, pp. 987–994, 2013.

[12] M. Choi, M. Humar, S. Kim, and S. H. Yun, "Step-index optical fiber made of biocompatible hydrogels," *Adv. Mater.*, vol. 27, pp. 4081–4086, 2015.

[13] S. Nizamoglu *et al.*, "Bioabsorbable polymer optical waveguides for deep-tissue photomedicine," *Nature Commun.*, vol. 7, no. 10374, pp. 1–7, 2016.

[14] D. Shan *et al.*, "Flexible biodegradable citrate-based polymeric step-index optical fiber," *Biomaterials*, vol. 143, pp. 142–148, 2017.

[15] R. Fu, W. Luo, R. Nazempour, D. Tan, H. Ding, and K. Zhang, "Implantable and biodegradable poly (l -lactic acid) fibers for optical neural interfaces," *Adv. Opt. Mater.*, vol. 6, no. 3, pp. 1–8, 2017.

[16] M. C. Hofmann *et al.*, "Scanning-fiber-based imaging method for tissue engineering," *J. Biomed. Opt.*, vol. 17, no. 6, 2012, Art. no. 066010.

[17] Y. M. Lin, A. R. Boccaccini, J. M. Polak, A. E. Bishop, and V. Maquet, "Biocompatibility of poly-DL-lactic acid (PDLLA) for lung tissue engineering," *J. Biomater. Appl.*, vol. 21, no. 2, pp. 109–18, 2006.

[18] B. C. Mack, K. W. Wright, and M. E. Davis, "A biodegradable filament for controlled drug delivery," *J. Controlled Release*, vol. 139, no. 3, pp. 205–211, 2009.

[19] F. Lin, X. Wang, Y. Wang, Y. Yang, and Y. Li, "Preparation and biocompatibility of electrospinning PDLLA/β-TCP/collagen for peripheral nerve regeneration," *RSC Adv.*, vol. 7, no. 66, pp. 41593–41602, 2017.

[20] R.-Y. Li, Z.-G. Liu, H.-Q. Liu, L. Chen, J.-F. Liu, and Y.-H. Pan, "Evaluation of biocompatibility and toxicity of biodegradable poly (DL-lactic acid) films," *Amer. J. Transl. Res.*, vol. 7, no. 8, pp. 1357–1370, 2015.

[21] Corbion, "Polymers for medical devices," 2018. [Online]. Available: https://www.corbion.com/static/downloads/datasheets/30d/PURASORB%20PDL%2020.pdf. Accessed on: Jul. 30, 2018.

[22] U.S. Food and Drug Administration, "Drug Master Files (DMFs)." [Online]. Available: https://www.fda.gov/downloads/drugs/developmentapprovalprocess/formssubmissionrequirements/drugmasterfilesdmfs/ucm370723.txt. Accessed on: Oct. 1, 2018.

[23] X. Liu, Y. Zou, W. Li, G. Cao, and W. Chen, "Kinetics of thermo-oxidative and thermal degradation of poly(d,l-lactide) (PDLLA) at processing temperature," *Polym. Degrad. Stab.*, vol. 91, no. 12, pp. 3259–3265, 2006.

[24] A. Rousseau and B. Boutevin, "Synthesis of low absportion halogenated polymers for POF," in *Proc. Plastic Opt. Fibres Appl. Conf.*, Paris, France, 1992, pp. 33–37.

[25] M. C. J. Large, L. Poladian, G. W. Barton, and M. A. van Eijkelenborg, "Fabrication of mPOFs," in *Microstructured Polymer Optical Fibres*. Berlin, Germany: Springer, 2007, pp. 103–104.

[26] M. G. Kuzyk, "Characterization techniques and properties," in *Polymer Fiber Optics: Materials, Physics, and Applications*. Boca Raton, FL, USA: CRC, 2007, pp. 153–168.

[27] A. Skumanich, M. Jurich, and J. D. Swalen, "Absorption and scattering in nonlinear optical polymeric systems," *Appl. Phys. Lett.*, vol. 62, no. 5, pp. 446–448, 1993.

[28] Z. Zhang, P. Zhao, P. Lin, and F. Sun, "Thermo-optic coefficients of polymers for optical waveguide applications," *Polymer*, vol. 47, no. 14, pp. 4893–4896, 2006.

[29] E. S. Kang, T. H. Lee, and B. S. Bae, "Measurement of the thermo-optic coefficients in sol-gel derived inorganic-organic hybrid material films," *Appl. Phys. Lett.*, vol. 81, no. 8, pp. 1438–1440, 2002.

[30] M. Beckers, T. Schlüter, T. Vad, T. Gries, and C.-A. Bunge, "An overview on fabrication methods for polymer optical fibers," *Polym. Int.*, vol. 64, no. 1, pp. 25–36, 2015.

[31] Thorlabs, Inc., "GIPOF120 – Graded-Index Perfluorinated POF, 120 μm core." [Online]. Available: https://www.thorlabs.com/thorproduct.cfm?partnumber=GIPOF120. Accessed on: Feb. 5, 2019.

[32] I. Bikandi, M. A. Illarramendi, G. Durana, G. Aldabaldetreku, and J. Zubia, "Spectral dependence of scattered light in step-index polymer optical fibers by side-illumination technique," *J. Light. Technol.*, vol. 32, no. 23, pp. 4539–4543, Dec. 2014.

[33] K. Shi *et al.*, "Synthesis, characterization, and application of reversible PDLLA-PEG-PDLLA copolymer thermogels in vitro and in vivo," *Sci. Rep.*, vol. 6, Jan. 2016, Art. no. 19077.

[34] I. Grizzi, H. Garreau, S. Li, and M. Vert, "Hydrolytic degradation of devices based on poly(dl-lactic acid) size-dependence," *Biomaterials*, vol. 16, no. 4, pp. 305–311, 1995.

[35] W. Heidemann *et al.*, "Degradation of poly(D,L)lactide implants with or without addition of calciumphosphates in vivo," *Biomaterials*, vol. 22, no. 17, pp. 2371–2381, 2001.

[36] Y. Tokiwa and T. Suzuki, "Hydrolysis of polyesters by lipases," *Nature*, vol. 270, pp. 76–78, 1977.

[37] M. A. Tracy *et al.*, "Factors affecting the degradation rate of poly(lactide-co-glycolide) microspheres in vivo and in vitro," *Biomaterials*, vol. 20, no. 11, pp. 1057–1062, 1999.

[38] L. Ferreira *et al.*, "Biocompatibility of chemoenzymatically derived dextran-acrylate hydrogels," *J. Biomed. Mater. Res. A*, vol. 68, pp. 584–596, 2004.

[39] A. C. Stähelin, A. Weiler, H. Rüfenacht, R. Hoffmann, A. Geissmann, and R. Feinstein, "Clinical degradation and biocompatibility of different bioabsorbable interference screws: A report of six cases," *Arthroscopy*, vol. 13, no. 2, pp. 238–244, 1997.

[40] *Optical Fibres – Part 1-40: Measurement Methods and Test Procedures – Attenuation*, IEC Standard 60793-1-40:2001, 2001.

[41] Y. Koike, "POF—From the past to the future," in *Proc. 7th Int. Plastic Opt. Fibres Conf.*, Berlin, Germany, 1998, p. 1–8.

[42] B. L. Wenig *et al.*, "Photodynamic therapy in the treatment of squamous cell carcinoma of the head and neck," *Arch. Otolaryngology—Head Neck Surg.*, vol. 116, no. 11, pp. 1267–1270, 1990.

[43] B. C. Wilson and M. S. Patterson, "The physics, biophysics and technology of photodynamic therapy," *Phys. Med. Biol.*, vol. 58, no. 9, pp. R61–R109, 2008.

[44] Industrial Fiber Optics, Inc., "Connector, SMA 905 POF 1 mm plastic optical fiber." [Online]. Available: http://i-fiberoptics.com/connector-detail.php?id=15&cat=pof. Accessed on: Dec. 20, 2018.

[45] O. Ziemann, J. Krauser, P. E. Zamzow, and W. Daum, "Simulation of optical waveguides," in *POF Handbook Optical Short Range Transmission Systems*. Berlin, Germany: Springer, 2008, pp. 763–801.

[46] W. M. Star, "Light delivery and light dosimetry for photodynamic therapy," *Lasers Med. Sci.*, vol. 5, no. 2, pp. 107–113, 1990.

[47] Y. Lin, S. Chen, M. Wang, and W. Liu, "Fiber-optic fast response pH sensor in fiber Bragg gating using intelligent hydrogel coatings," *Opt. Eng.*, vol. 54, no. 5, p. 57107, 2015.

Authors' biographies not available at the time of publication.